Received: 26 August 2020 | Revised: 29 March 2021 | Accepted: 6 April 2021

DOI: 10.1002/zamm.202000232

ZAMM

ORIGINAL PAPER

Vector solitons for the (2 + 1)-dimensional coupled nonlinear Schrödinger system in the Kerr nonlinear optical fiber

Yan Sun[1,2] | **Bo Tian**[1,2] | **Qi-Xing Qu**[3] | **Han-Peng Chai**[1,2] | **Yu-Qiang Yuan**[1,2] | **Wen-Rui Shan**[1,2] | **Yan Jiang**[1,2]

[1] State Key Laboratory of Information Photonics and Optical Communications, Beijing University of Posts and Telecommunications, Beijing 100876, China

[2] School of Science, Beijing University of Posts and Telecommunications, Beijing 100876, China

[3] School of Information, University of International Business and Economics, Beijing 100029, China

Correspondence
Bo Tian, State Key Laboratory of Information Photonics and Optical Communications, and School of Science, Beijing University of Posts and Telecommunications, Beijing 100876, China.
Email: tian_bupt@163.com

Funding information
National Natural Science Foundation of China, Grant/Award Numbers: 11772017, 11805020, 11272023, 11471050; Fund of State Key Laboratory of Information Photonics and Optical Communications, Grant/Award Number: IPOC: 2017ZZ05; Fundamental Research Funds for the Central Universities of China, Grant/Award Number: 2011BUPTYB02; Fundamental Research Funds for the Central Universities in UIBE, Grant/Award Number: CXTD12-04

Investigated in this paper is the $(2+1)$-dimensional coupled nonlinear Schrödinger system, which describes the propagation of the optical soliton through the Kerr nonlinear fiber in which each component diffracts in two transverse dimensions. By virtue of the Kadomtsev-Petviashvili hierarchy reduction, we obtain the bright, dark and mixed vector soliton solutions in terms of the Gramian. We investigate the vector solitons graphically: (1) Bright-dark one solitons with one of the components being gray or black are shown. Bouncing, beating, oscillating and breathing effects which appear during the interactions between the bright-dark two solitons are discussed, and those interactions are shape-preserving; (2) Degenerate and non-degenerate dark-dark one solitons are presented. Interaction of the dark-dark two solitons is discussed and the two solitons keep their amplitudes and velocities invariant except for some phase shifts during the interaction; (3) Bound-state and complexes of the bright-bright solitons are presented.

KEYWORDS
interactions, Kerr nonlinear optical fiber, Kadomtsev-Petviashvili hierarchy reduction, vector solitons, $(2+1)$-dimensional coupled nonlinear Schrödinger system

1 | INTRODUCTION

It has been seen that the optical solitons arise due to the self-phase modulation in balancing the group velocity dispersion, and the interaction of the scalar solitons in the nonlinear optical fibers has been described by the nonlinear Schrödinger (NLS)-type equations for scalar fields [1–11]. Experiments of the optical fiber have also been studied [12–14]. Relevant soliton issues can be seen in Refs. [15–28]. In the multimode and birefringent fibers, vector optical solitons for the coupled NLS (CNLS) equations have been considered in two (or more) field components with different frequencies or polarizations [29–37]. Particularly, dark-dark and bright-bright solitons have been proved to be stable under small perturbations experimentally and numerically, while bright-dark solitons have been displayed that they are stable only under certain situations [29]. Interactions between vector solitons have applications in logic gates and optical computation [38]. In comparison to the scalar optical solitons, mutually self-trap vector optical solitons (temporal or spatial) have emerged due to the interplay between dispersive (temporal) or diffractive (spatial) effects and nonlinear effects [39,40]. For example, researchers have considered the Manakov system [34,41–48]

$$iE_{1Z} + E_{1TT} + \chi(|E_1|^2 + |E_2|^2)E_1 = 0, \tag{1a}$$

$$iE_{2Z} + E_{2TT} + \chi(|E_1|^2 + |E_2|^2)E_2 = 0, \tag{1b}$$

where E_1 and E_2 are the slowly varying envelopes of the two interacting optical modes, χ is the strength of the nonlinearity, Z and T represent the normalized distance along the direction of the propagation and the retarded time [45]. Moreover, T has been replaced by the transverse coordinate X when people discuss the spatial solitons [45]. Spatial solitons of System (1) in the AlGaAs planar waveguides have been obtained experimentally [46]. Conditions have been established for the soliton switching and energy coupling among the two modes in a nonlinear optical fiber [47]. System (1) has been proved to support the bright-bright, bright-dark and dark-dark solitons [48].

When the spatial solitons are extended to the $(2 + 1)$-dimensional geometry with each component diffracted in two transverse dimensions, researchers have focused their attention on the following $(2 + 1)$-dimensional CNLS system in the Kerr nonlinear optical fiber [49–51]:

$$i\psi_t + \psi_{xx} + \psi_{yy} + \sigma(|\psi|^2 + \alpha|\phi|^2)\psi = 0, \tag{2a}$$

$$i\phi_t + \phi_{xx} + \phi_{yy} + \sigma(\alpha|\psi|^2 + |\phi|^2)\phi = 0, \tag{2b}$$

where the slowly varying envelopes ψ and ϕ are the complex functions of the retarded time t and transverse coordinates x and y, α is a real constant which measures the relative strength of cross-phase modulation and self-phase modulation, and has been influenced by the polarization of the beams, nonlinearity and anisotropy of the fiber [50]. The value of α varies over a wide range: $\alpha \geq 2/3$ corresponds to the Kerr-type electronic nonlinearity, whereas $\alpha \leq 7$ corresponds to the nonlinearity resulting from the molecular orientation [49]. When $\sigma = 1$, System (2) is self-focusing which have been proved to support the bright-bright and bright-dark solitons [49,51]; When $\sigma = -1$, System (2) is self-defocusing which have been proved to support the bright-dark and dark-dark solitons [51]. Existence and stability of the vector solitons formed by two incoherently interacting optical beams in the bulk Kerr and saturable medium with $\sigma = 1$ have been discussed [50]. Interaction between the bright-bright solitons for System (2) with $\alpha = 1$ has been studied [49].

To our knowledge, bright-dark and dark-dark solitons for System (2) with $\alpha = 1$ have not been investigated. Moreover, bound-state bright-bright solitons and soliton complexes for System (2) have not been studied yet. In this paper, we will work on the bright, dark and mixed vector soliton solutions for System (2) via the Kadomtsev-Petviashvili (KP) hierarchy reduction[1]. Bright-dark soliton solutions in terms of the Gramian for System (2) will be given in Section 2 and interaction between the bright-dark solitons will be studied. Section 3 will be devoted to the dark-dark soliton solutions in terms of the Gramian for System (2) and interaction properties of the dark-dark solitons will be studied. Bright-bright soliton solutions in terms of the Gramian for System (2) will be derived and propagation of the bound-state bright-bright solitons and soliton complexes will be derived in Section 4. Section 5 will be our conclusions.

2 | BRIGHT-DARK SOLITON SOLUTIONS AND SOLITON INTERACTION FOR SYSTEM (2)

2.1 | Bright-dark soliton solutions for System (2)

Under the variable transformations

$$\psi = e^{-i|\rho|^2 t}\frac{g}{f}, \quad \phi = \rho e^{i\left[(\gamma_1 x + \gamma_2 y) - (|\rho|^2 + \gamma_1^2 + \gamma_2^2)t\right]}\frac{h}{f},$$

[1] The KP hierarchy reduction has been used to derive the vector soliton solutions for the Manakov system [34], vector NLS equations [36], Yajima-Oikawa System [53] and AB system [54].

with $\sigma = -1$, System (2) can be transformed into

$$(iD_t + D_x^2 + D_y^2)g \cdot f = 0, \tag{3a}$$

$$(iD_t + D_x^2 + D_y^2 + 2i\gamma_1 D_x + 2i\gamma_2 D_y)h \cdot f = 0, \tag{3b}$$

$$(D_x^2 + D_y^2)f \cdot f - |\rho|^2 f^2 = -\left(|g|^2 + |\rho|^2|h|^2\right), \tag{3c}$$

where γ_1 and γ_2 are the real constants, ρ is a complex constant, g and h are the complex functions of x, y and t, f is a real function of x, y and t, D_x, D_y and D_t are the Hirota bilinear differential operators defined by [55]

$$D_x^{\chi_1} D_y^{\chi_2} D_t^{\chi_3}(F \cdot G) = \left(\frac{\partial}{\partial x} - \frac{\partial}{\partial x'}\right)^{\chi_1} \left(\frac{\partial}{\partial y} - \frac{\partial}{\partial y'}\right)^{\chi_2} \left(\frac{\partial}{\partial t} - \frac{\partial}{\partial t'}\right)^{\chi_3} F(x, y, t)G(x', y', t')|_{x'=x, y'=y, t'=t},$$

with χ_1, χ_2 and χ_3 being the non-negative integers, F as a function of x, y and t, G as a function of the formal variables x', y' and t'.

N-bright-dark soliton solutions in terms of the Gramian for System (2) are

$$\psi = e^{-i|\rho|^2 t} \frac{g}{f}, \quad \phi = \rho e^{i[(\gamma_1 x + \gamma_2 y) - (|\rho|^2 + \gamma_1^2 + \gamma_2^2)t]} \frac{h}{f}, \tag{4}$$

where

$$f = \begin{vmatrix} \mathbf{A} & \mathbf{I} \\ -\mathbf{I} & \mathbf{B} \end{vmatrix}, \quad g = \begin{vmatrix} \mathbf{A} & \mathbf{I} & \mathbf{\Phi}^T \\ -\mathbf{I} & \mathbf{B} & \mathbf{0}^T \\ \mathbf{0} & \mathbf{\Psi} & 0 \end{vmatrix}, \quad h = \begin{vmatrix} \mathbf{R} & \mathbf{I} \\ -\mathbf{I} & \mathbf{B} \end{vmatrix},$$

$\mathbf{I}$ is the $N \times N$ identity matrix, $\mathbf{0}$ is the $1 \times N$ zero matrix, the superscript T means the transpose of the matrix, $\mathbf{A}$, $\mathbf{B}$ and $\mathbf{R}$ are all the $N \times N$ matrices whose elements are a_{mn}'s, b_{mn}'s and r_{mn}'s $(1 \le m, n \le N)$, m, n and N are all the positive integers, $\mathbf{\Phi}$ and $\mathbf{\Psi}$ are the $1 \times N$ matrices with

$$a_{mn} = \frac{1}{p_m + p_n^*} e^{\xi_m + \xi_n^*}, \quad b_{mn} = \frac{\tilde{\alpha}_m^* \tilde{\alpha}_n \Delta_m \Delta_n^*}{(p_n + p_m^*)(|\rho|^2 - 2\Delta_m \Delta_n^*)}, \quad r_{mn} = -\frac{\Delta_m}{\Delta_n^*} a_{mn},$$

$$\mathbf{\Psi} = -(\tilde{\alpha}_1, \tilde{\alpha}_2, \dots, \tilde{\alpha}_N), \quad \mathbf{\Phi} = (e^{\xi_1}, e^{\xi_2}, \dots, e^{\xi_N}),$$

$$\Delta_n = p_n - i(k\gamma_1 + l\gamma_2), \quad \xi_n = p_n(kx + ly) + ip_n^2 t + \xi_{n0},$$

k and l being the real constants which satisfy $k^2 + l^2 = 1$, "$*$" representing the complex conjugation, p_n's, $\tilde{\alpha}_n$'s and ξ_{n0}'s as the complex constants.

Setting $N = 1$ in Solutions (4), we derive the bright-dark one-soliton solutions for System (2),

$$\phi = \tilde{\alpha}_1 \sqrt{\frac{p_1 + p_1^*}{b_{11}}} e^{\frac{\xi_1 - \xi_1^* - 2i|\rho|^2 t}{2}} \operatorname{sech}\left(\frac{\xi_1 + \xi_1^* + \ln \frac{b_{11}}{p_1 + p_1^*}}{2}\right), \tag{5a}$$

$$\psi = \frac{\rho}{2} e^{i(\gamma_1 x + \gamma_2 y) - i(|\rho|^2 + \gamma_1^2 + \gamma_2^2)t} \left[1 - \frac{\Delta_1}{\Delta_1^*} - \left(1 + \frac{\Delta_1}{\Delta_1^*}\right) \tanh\left(\frac{\xi_1 + \xi_1^* + \ln \frac{b_{11}}{p_1 + p_1^*}}{2}\right)\right], \tag{5b}$$

with $(p_1+p_1^*)b_{11}>0$. The amplitudes of ψ and ϕ are given by

$$A_1=(p_1+p_1^*)\sqrt{\left|\frac{\rho}{\Delta_1}\right|^2-2},\quad A_2=\frac{|\rho|}{2}\left(2-\frac{p_1+p_1^*}{|\Delta_1|}\right),$$

which are affected by ρ, p_1 and Δ_1.

Setting $N=2$ in Solutions (4), we derive the bright-dark two-soliton solutions for System (2),

$$\psi=e^{-i|\rho|^2t}\frac{g}{f},\quad \phi=\rho e^{i(\gamma_1x+\gamma_2y)-i(|\rho|^2+\gamma_1^2+\gamma_2^2)t}\frac{h}{f},\tag{6}$$

where

$$\begin{aligned}
f&=1+e^{\xi_1+\xi_1^*+\omega_{11}}+e^{\xi_1+\xi_2^*+\omega_0}+e^{\xi_2+\xi_1^*+\omega_0^*}+e^{\xi_2+\xi_2^*+\omega_{22}}+e^{\xi_1+\xi_1^*+\xi_2+\xi_2^*+\omega_{33}},\\
g&=\tilde{\alpha}_1e^{\xi_1}+\tilde{\alpha}_2e^{\xi_2}+e^{\xi_1+\xi_2+\xi_1^*+\omega_{12}}+e^{\xi_1+\xi_2+\xi_2^*+\omega_{21}},\\
h&=1+\sigma_{11}e^{\xi_1+\xi_1^*+\omega_{11}}+\sigma_{12}e^{\xi_1+\xi_2^*+\omega_0}+\sigma_{21}e^{\xi_2+\xi_1^*+\omega_0^*}\\
&\quad+\sigma_{22}e^{\xi_2+\xi_2^*+\omega_{22}}+\sigma_{11}\sigma_{22}e^{\xi_1+\xi_1^*+\xi_2+\xi_2^*+\omega_{33}},
\end{aligned}$$

with

$$\begin{aligned}
&e^{\omega_{11}}=\frac{b_{11}}{p_1+p_1^*},\quad e^{\omega_0}=\frac{b_{21}}{p_1+p_2^*},\quad e^{\omega_{22}}=\frac{b_{22}}{p_2+p_2^*},\\
&e^{\omega_{12}}=\frac{p_1-p_2}{(p_1+p_1^*)(p_2+p_1^*)}(\tilde{\alpha}_1b_{12}-\tilde{\alpha}_2b_{11}),\quad e^{\omega_{21}}=\frac{p_2-p_1}{(p_1+p_2^*)(p_2+p_2^*)}(\tilde{\alpha}_2b_{21}-\tilde{\alpha}_1b_{22}),\\
&e^{\omega_{33}}=\frac{|p_1-p_2|^2}{(p_1+p_1^*)(p_2+p_2^*)|p_1+p_2^*|^2}(b_{11}b_{22}-b_{12}b_{21}),\quad \sigma_{mn}=-\frac{\Delta_m}{\Delta_n^*},
\end{aligned}$$

under $b_{11}(p_1+p_1^*)>0$ and $b_{22}(p_2+p_2^*)>0$.

According to Solutions (4), we set $N=3$ and derive the bright-dark three-soliton solutions for System (2) with

$$f=\begin{vmatrix}
a_{11}&a_{12}&a_{13}&1&0&0\\
a_{21}&a_{22}&a_{23}&0&1&0\\
a_{31}&a_{32}&a_{33}&0&0&1\\
-1&0&0&b_{11}&b_{12}&b_{13}\\
0&-1&0&b_{21}&b_{22}&b_{23}\\
0&0&-1&b_{31}&b_{32}&b_{33}
\end{vmatrix},\quad g=\begin{vmatrix}
a_{11}&a_{12}&a_{13}&1&0&0&e^{\xi_1}\\
a_{21}&a_{22}&a_{23}&0&1&0&e^{\xi_2}\\
a_{31}&a_{32}&a_{33}&0&0&1&e^{\xi_3}\\
-1&0&0&b_{11}&b_{12}&b_{13}&0\\
0&-1&0&b_{21}&b_{22}&b_{23}&0\\
0&0&-1&b_{31}&b_{32}&b_{33}&0\\
0&0&0&-\tilde{\alpha}_1&-\tilde{\alpha}_2&-\tilde{\alpha}_3&0
\end{vmatrix},$$

$$h=\begin{vmatrix}
-\frac{\Delta_1}{\Delta_1^*}a_{11}&-\frac{\Delta_1}{\Delta_2^*}a_{12}&-\frac{\Delta_1}{\Delta_3^*}a_{13}&1&0&0\\
-\frac{\Delta_2}{\Delta_1^*}a_{21}&-\frac{\Delta_2}{\Delta_2^*}a_{22}&-\frac{\Delta_2}{\Delta_3^*}a_{23}&0&1&0\\
-\frac{\Delta_3}{\Delta_1^*}a_{31}&-\frac{\Delta_3}{\Delta_2^*}a_{32}&-\frac{\Delta_3}{\Delta_3^*}a_{33}&0&0&1\\
-1&0&0&b_{11}&b_{12}&b_{13}\\
0&-1&0&b_{21}&b_{22}&b_{23}\\
0&0&-1&b_{31}&b_{32}&b_{33}
\end{vmatrix}.$$

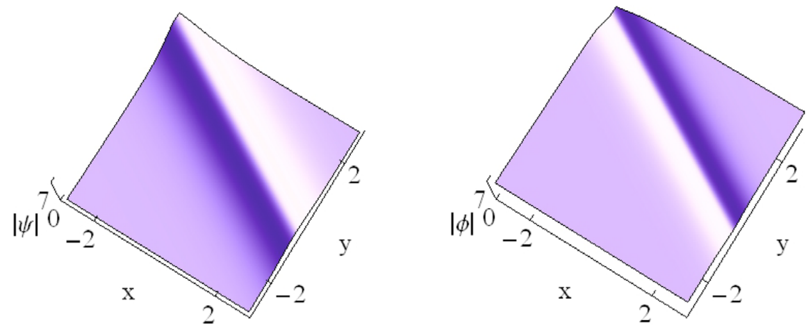

FIGURE 1 Bright-dark one soliton via Solutions (5) at $t = 0$ with $\rho = 6$, $p_1 = 2$, $\gamma_1 = -2$, $\gamma_2 = -1$, $k = 0.5$, $l = \frac{\sqrt{3}}{2}$, $\xi_{10} = 0$ and $\tilde{\alpha}_1 = 1$

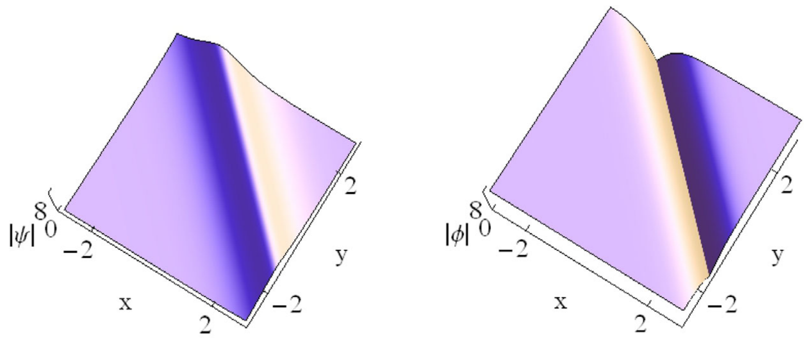

FIGURE 2 The same as Figure 1 except that $\rho = 8$, $p_1 = 2.2 + i$, $\gamma_1 = \gamma_2 = \frac{\sqrt{2}}{2}$, $k = l = \frac{\sqrt{2}}{2}$

2.2 | Discussion on the bright-dark solitons for System (2)

Figures 1 and 2 depict the bright-dark one solitons via Solutions (5). Figure 1 shows the ϕ component of the soliton is gray with $\Delta_1 \neq \Delta_1^*$. When $\Delta_1 = \Delta_1^*$, the minimum intensity for the ϕ component drops to zero and the ϕ component of the soliton is black, as seen in Figure 2.

Figure 3 depicts the interactions between the bright-dark two solitons via Solutions (6). In Figure 3a, two solitons experience a phase shift and form a well around the interaction area upon their mutual interaction. After the interaction, the two solitons keep their amplitudes and velocities invariant. In Figure 3b, bouncing effect emerges with $p_{1R} = p_{2R}$, the two solitons do not achieve the maximum, unlike the phenomenon in Figure 3a.

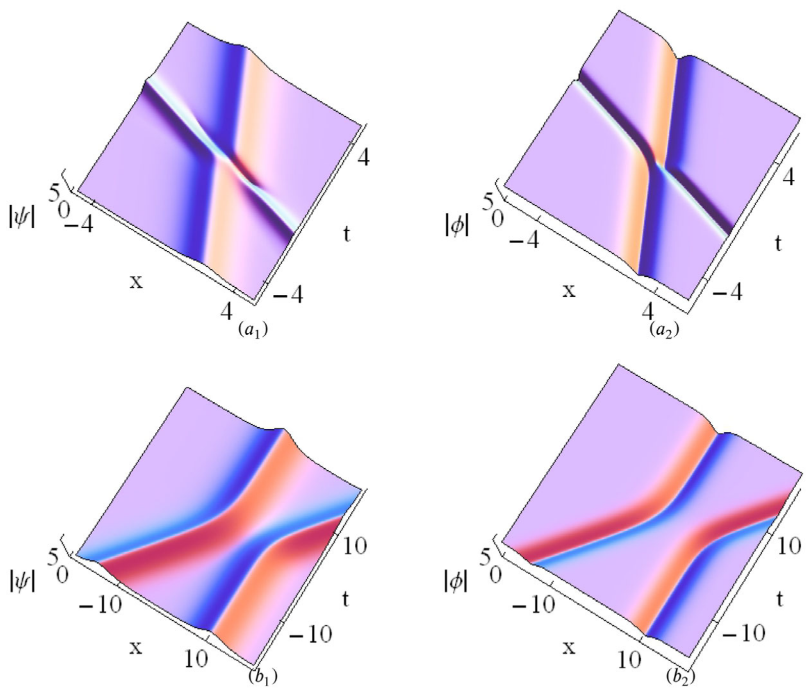

FIGURE 3 Interactions between the bright-dark two solitons via Solutions (6) at $y = 0$ with $\rho = 4$. (a) $\gamma_1 = 2$, $\gamma_2 = -1$, $k = l = -\frac{2}{2}$, $\xi_{10} = 1$, $\tilde{\alpha}_1 = 2$, $\tilde{\alpha}_2 = 1 + 1.5i$, $p_1 = -1.8 + 1.2i$ and $p_2 = -2.2 + 0.1667i$, (b) $\gamma_1 = \frac{1}{2}$, $\gamma_2 = -1$, $k = \frac{1}{2}$, $l = \frac{\sqrt{3}}{2}$, $\xi_{10} = 0$, $\tilde{\alpha}_1 = \tilde{\alpha}_2 = 2 + i$, $p_1 = 1 + 0.2i$ and $p_2 = 1$

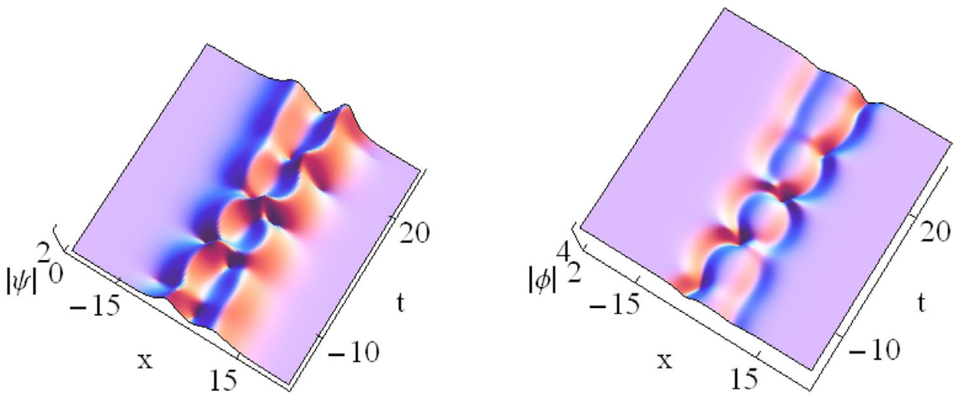

FIGURE 4 Beating effect between the bright-dark two solitons via Solutions (6) at $y = 0$ with $\rho = 4, \gamma_1 = 1, \gamma_2 = 1.5, p_1 = 1 + 0.02i$, $p_2 = 0.7 - 0.02i, k = 0.5, l = \frac{\sqrt{3}}{2}, \xi_{10} = 1$ and $\tilde{\alpha}_1 = \tilde{\alpha}_2 = 1 + i$

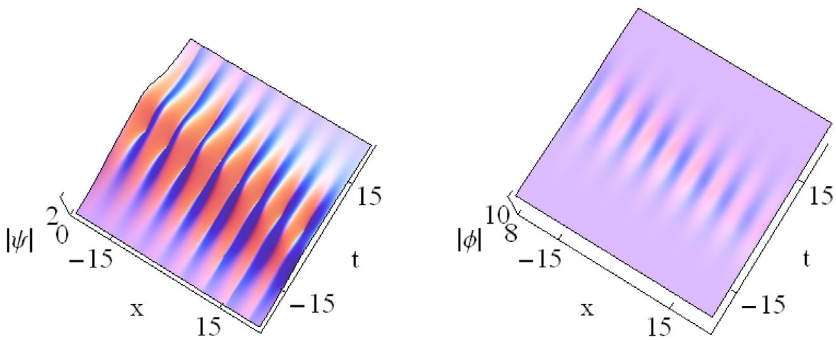

FIGURE 5 Oscillating effect between the bright-dark two solitons via Solutions (6) at $y = 0$ with $\rho = 10, \gamma_1 = 0.1, \gamma_2 = 0.1$, $p_1 = 0.0625 + i, p_2 = -0.1 - i, k = \frac{1}{2}, l = \frac{\sqrt{3}}{2}$, $\xi_{10} = 0.5$ and $\tilde{\alpha}_1 = \tilde{\alpha}_2 = 1$

When $p_{1\mathrm{I}} = -p_{2\mathrm{I}} \ll 1$ ($p_{j\mathrm{I}}$ as the imaginary part of p_j), beating effect appears during the interaction between the bright-dark two solitons, as seen in Figure 4. The bright-dark two solitons form a bound mode when $t \to 0$, indicating the amount of energy carried in the bound mode [37]. When $t \to \pm\infty$, the bright-dark two solitons separate gradually and the beating effect becomes weaken.

Figure 5 depicts the oscillating effect during the interaction between the bright-dark two solitons. Oscillating effect enhances around the interaction area and amplitudes of ψ and ϕ components around the interaction area achieve the maximum. Interaction is elastic, as the profiles of the solitons remain the same before and after the interaction.

Figure 6 depicts the breathing effect which appears during the interaction between the bright-dark two solitons. In Figure 6a, the bright-dark two solitons attract and repel each other periodically since the velocities of the two solitons are the same with $p_{1\mathrm{I}} = p_{2\mathrm{I}}$. When $p_{1\mathrm{I}} = p_{2\mathrm{I}} = 0$, the stationary bound-state bright-dark two solitons are presented in Figure 6b, and they evolve periodically along the t axis. Figures 6 (a_3), 6(a_4), 6(b_3) and 6(b_4) are density plots.

3 | DARK-DARK SOLITON SOLUTIONS AND SOLITON INTERACTION FOR SYSTEM (2)

3.1 | Dark-dark soliton solutions for System (2)

Under the variable transformations

$$\psi = \mu e^{i\left[(\alpha_1 x + \alpha_2 y) - (|\mu|^2 + |\nu|^2 + \alpha_1^2 + \alpha_2^2)t\right]} \frac{g}{f},$$

$$\phi = \nu e^{i\left[(\beta_1 x + \beta_2 y) - (|\mu|^2 + |\nu|^2 + \beta_1^2 + \beta_2^2)t\right]} \frac{h}{f},$$

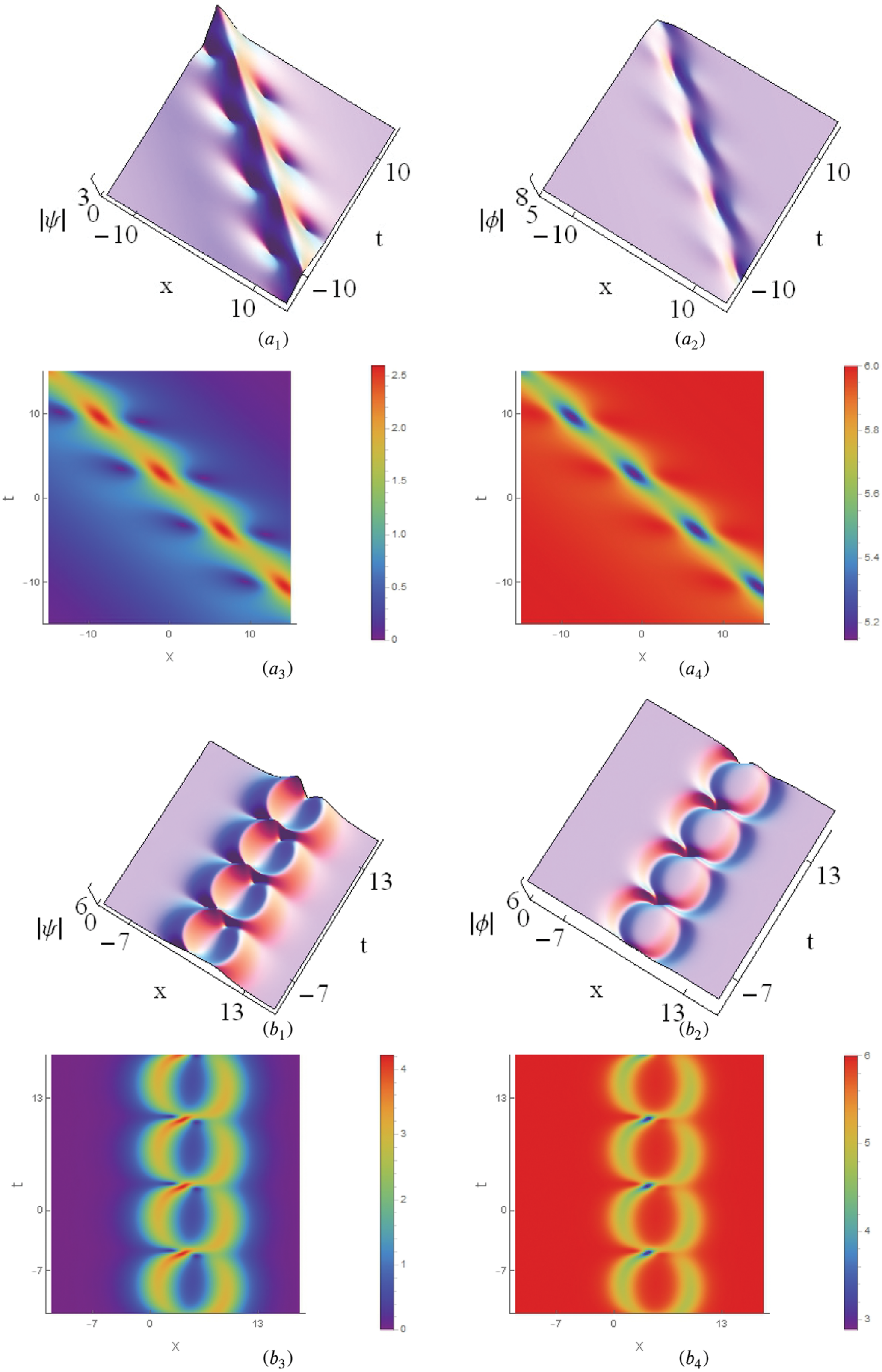

FIGURE 6 Breathing effects between the bright-dark two solitons via Solutions (6) at $y = 0$ with $\rho = 6, \gamma_1 = 1, \gamma_2 = \frac{3}{2}, k = \frac{1}{2}, l = \frac{\sqrt{3}}{2}$, $\xi_{10} = 0, \tilde{\alpha}_1 = 1 + i$ and $\tilde{\alpha}_2 = 2 + 0.3i$. (a) Bound-state solitons: $p_1 = 1 - 0.2857i$, $p_2 = 0.25 - 0.2857i$, (b) Stationary bound-state solitons: $p_1 = 1.5$, $p_2 = 1.2$

with $\sigma = -1$, System (2) can be transformed into

$$(iD_t + D_x^2 + D_y^2 + 2i\alpha_1 D_x + 2i\alpha_2 D_y)g \cdot f = 0, \tag{7a}$$

$$(iD_t + D_x^2 + D_y^2 + 2i\beta_1 D_x + 2i\beta_2 D_y)h \cdot f = 0, \tag{7b}$$

$$(D_x^2 + D_y^2)f \cdot f - \left(|\mu|^2 + |\nu|^2\right)f^2 = -\left(|\mu|^2|g|^2 + |\nu|^2|h|^2\right), \tag{7c}$$

where α_1, α_2, β_1 and β_2 are the real constants, μ and ν are the complex constants.

N-dark-dark soliton solutions in terms of the Gramian for System (2) are

$$\psi = \mu e^{i\left[(\alpha_1 x+\alpha_2 y)-(|\mu|^2+|\nu|^2+\alpha_1^2+\alpha_2^2)t\right]}\frac{g}{f}, \quad \phi = \nu e^{i\left[(\beta_1 x+\beta_2 y)-(|\mu|^2+|\nu|^2+\beta_1^2+\beta_2^2)t\right]}\frac{h}{f}, \tag{8}$$

where

$$f = |\mathbf{I} + \mathbf{A}|, \quad g = |\mathbf{I} + \mathbf{W}|, \quad h = |\mathbf{I} + \mathbf{V}|,$$

W and **V** are both the $N \times N$ matrices whose elements are w_{mn}'s and v_{mn}'s with

$$w_{mn} = -\frac{\varrho_m}{\varrho_n^*}a_{mn}, \quad v_{mn} = -\frac{\tilde{\varrho}_m}{\tilde{\varrho}_n^*}a_{mn}, \quad a_{mn} = \frac{1}{p_m + p_n^*}e^{\xi_m+\xi_n^*},$$

$$\varrho_n = p_n - i(k\alpha_1 + l\alpha_2), \quad \tilde{\varrho}_n = p_n - i(k\beta_1 + l\beta_2),$$

$$\xi_n = p_n(kx + ly) + ip_n^2 t + \xi_{n0},$$

which satisfy $k^2 + l^2 = 1$, and p_n's, α_n's, ξ_{n0}'s satisfy

$$\frac{|\mu|^2}{\left|p_j - i(k\alpha_1 + l\alpha_2)\right|^2} + \frac{|\nu|^2}{\left|p_j - i(k\beta_1 + l\beta_2)\right|^2} = 2. \tag{9}$$

Setting $N = 1$ in Solutions (8), we derive the dark-dark one-soliton solutions for System (2),

$$\psi = \mu e^{i\left[(\alpha_1 x+\alpha_2 y)-(|\mu|^2+|\nu|^2+\alpha_1^2+\alpha_2^2)t\right]}\left[\frac{-\varrho_{1I}}{\varrho_1^*} + \frac{\varrho_{1R}}{\varrho_1^*}\tanh\left(\frac{\xi_1 + \xi_1^* + \ln\frac{1}{p_1+p_1^*}}{2}\right)\right], \tag{10a}$$

$$\phi = \nu e^{i\left[(\beta_1 x+\beta_2 y)-(|\mu|^2+|\nu|^2+\beta_1^2+\beta_2^2)t\right]}\left[\frac{-\tilde{\varrho}_{1I}}{\tilde{\varrho}_1^*} + \frac{\tilde{\varrho}_{1R}}{\tilde{\varrho}_1^*}\tanh\left(\frac{\xi_1 + \xi_1^* + \ln\frac{1}{p_1+p_1^*}}{2}\right)\right], \tag{10b}$$

under (9), where the subscript R denotes the real part of the complex constant. In addition, we require that $p_1 + p_1^* > 0$ to avoid the singularity. Amplitudes of the ψ and ϕ components are given by

$$B_1 = \left|\mu\frac{\varrho_1}{\varrho_1^*}\right|, \quad B_2 = \left|\nu\frac{\tilde{\varrho}_1}{\tilde{\varrho}_1^*}\right|,$$

which are affected by μ, ν, ϱ_1 and $\tilde{\varrho}_1$.

Setting $N = 2$ in Solutions (8), we derive the dark-dark two-soliton solutions for System (2),

$$\psi = \mu e^{i\left[(\alpha_1 x+\alpha_2 y)-(|\mu|^2+|\nu|^2+\alpha_1^2+\alpha_2^2)t\right]}\frac{g}{f}, \quad \phi = \nu e^{i\left[(\beta_1 x+\beta_2 y)-(|\mu|^2+|\nu|^2+\beta_1^2+\beta_2^2)t\right]}\frac{h}{f}, \tag{11}$$

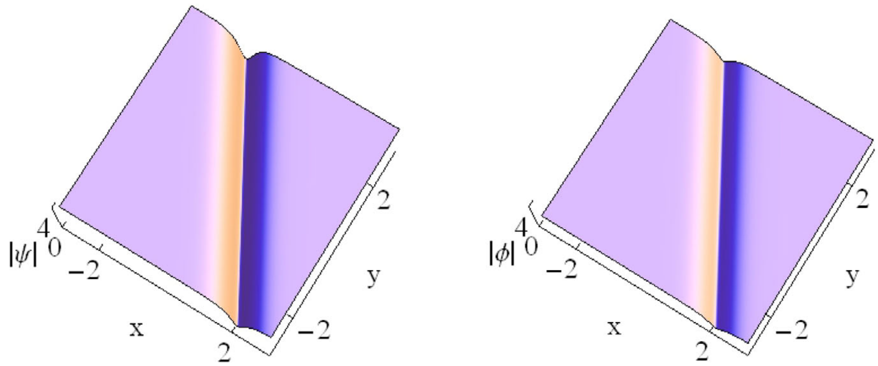

FIGURE 7 Degenerate dark-dark one soliton via Solutions (8) at $t = 0$ with $\mu = 4$, $\nu = 2$, $p_1 = 3 + 3i$, $\alpha_1 = 2\sqrt{3}$, $\alpha_2 = 2$, $\beta_1 = \sqrt{3}$, $\beta_2 = 5$, $k = \frac{\sqrt{3}}{2}$, $\alpha_1 = \frac{1}{2}$ and $\xi_{10} = 0$

where

$$f = 1 + e^{\xi_1+\xi_1^*+\tilde{\omega}_1} + e^{\xi_2+\xi_2^*+\tilde{\omega}_2} + e^{\xi_1+\xi_1^*+\xi_2+\xi_2^*+\tilde{\omega}_3},$$

$$g = 1 - \frac{\varrho_1}{\varrho_1^*}e^{\xi_1+\xi_1^*+\tilde{\omega}_1} - \frac{\varrho_2}{\varrho_2^*}e^{\xi_2+\xi_2^*+\tilde{\omega}_2} + \frac{\varrho_1\varrho_2}{\varrho_1^*\varrho_2^*}e^{\xi_1+\xi_1^*+\xi_2+\xi_2^*+\tilde{\omega}_3},$$

$$h = 1 - \frac{\tilde{\varrho}_1}{\tilde{\varrho}_1^*}e^{\xi_1+\xi_1^*+\tilde{\omega}_1} - \frac{\tilde{\varrho}_2}{\tilde{\varrho}_2^*}e^{\xi_2+\xi_2^*+\tilde{\omega}_2} + \frac{\tilde{\varrho}_1\tilde{\varrho}_2}{\tilde{\varrho}_1^*\tilde{\varrho}_2^*}e^{\xi_1+\xi_1^*+\xi_2+\xi_2^*+\tilde{\omega}_3},$$

with

$$e^{\tilde{\omega}_1} = \frac{1}{p_1 + p_1^*}, \quad e^{\tilde{\omega}_2} = \frac{1}{p_2 + p_2^*}, \quad e^{\tilde{\omega}_3} = \frac{|p_1 - p_2|^2}{(p_1 + p_1^*)(p_2 + p_2^*)|p_1 + p_2^*|^2},$$

under $p_1 + p_1^* > 0$, $p_2 + p_2^* > 0$ and (9).

Likewise, setting $N = 3$ in Solutions (8), we derive the dark-dark three-soliton solutions for System (2) with

$$f = \begin{vmatrix} 1 + a_{11} & a_{12} & a_{13} \\ a_{21} & 1 + a_{22} & a_{23} \\ a_{31} & a_{32} & 1 + a_{33} \end{vmatrix},$$

$$g = \begin{vmatrix} 1 - \frac{\varrho_1}{\varrho_1^*}a_{11} & -\frac{\varrho_1}{\varrho_2^*}a_{12} & -\frac{\varrho_1}{\varrho_3^*}a_{13} \\ -\frac{\varrho_2}{\varrho_1^*}a_{21} & 1 - \frac{\varrho_2}{\varrho_2^*}a_{22} & -\frac{\varrho_2}{\varrho_2^*}a_{23} \\ -\frac{\varrho_3}{\varrho_1^*}a_{31} & -\frac{\varrho_3}{\varrho_2^*}a_{32} & 1 - \frac{\varrho_3}{\varrho_3^*}a_{33} \end{vmatrix},$$

$$h = \begin{vmatrix} 1 - \frac{\tilde{\varrho}_1}{\tilde{\varrho}_1^*}a_{11} & -\frac{\tilde{\varrho}_1}{\tilde{\varrho}_2^*}a_{12} & -\frac{\tilde{\varrho}_1}{\tilde{\varrho}_3^*}a_{13} \\ -\frac{\tilde{\varrho}_2}{\tilde{\varrho}_1^*}a_{21} & 1 - \frac{\tilde{\varrho}_2}{\tilde{\varrho}_2^*}a_{22} & -\frac{\tilde{\varrho}_2}{\tilde{\varrho}_2^*}a_{23} \\ -\frac{\tilde{\varrho}_3}{\tilde{\varrho}_1^*}a_{31} & -\frac{\tilde{\varrho}_3}{\tilde{\varrho}_2^*}a_{32} & 1 - \frac{\tilde{\varrho}_3}{\tilde{\varrho}_3^*}a_{33} \end{vmatrix}.$$

3.2 | Discussion on the dark-dark solitons for System (2)

Figures 7 and 8 depict the degenerate and non-degenerate dark-dark one solitons via Solutions (8). We can observe that the minimum intensities for the ψ and ϕ components drop to zero simultaneously only when $k\alpha_1 + l\alpha_2 = k\beta_1 + l\beta_2$.

Figure 9 depicts the interaction between the dark-dark two solitons via Solutions (10). During the interaction, the two solitons keep their amplitudes and velocities invariant except for some phase shifts. Figure 9b is the density plot of the Figure 9a.

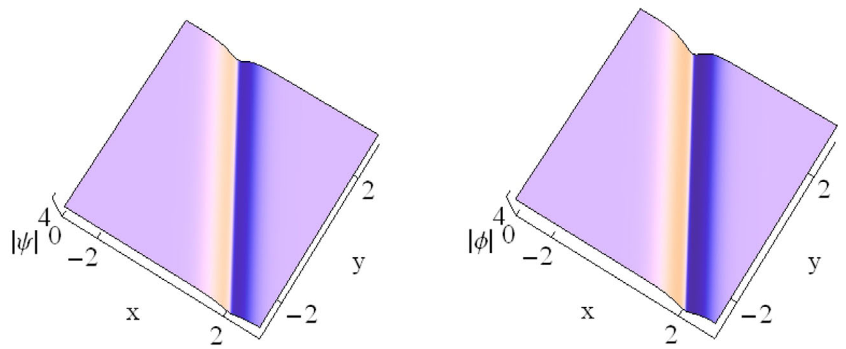

FIGURE 8 Non-degenerate dark-dark one soliton via Solutions (8) at $t = 0$ with $\mu = 3$, $\nu = \sqrt{\frac{10(2307-578\sqrt{3})}{1201}}$, $p_1 = 2.5 + 2.5i$, $\alpha_1 = 1$, $\alpha_2 = 3\sqrt{3}$, $\beta_1 = 1$, $\beta_2 = 1$, $k = \frac{\sqrt{3}}{2}$, $l = 0.5$ and $\xi_{10} = 0$

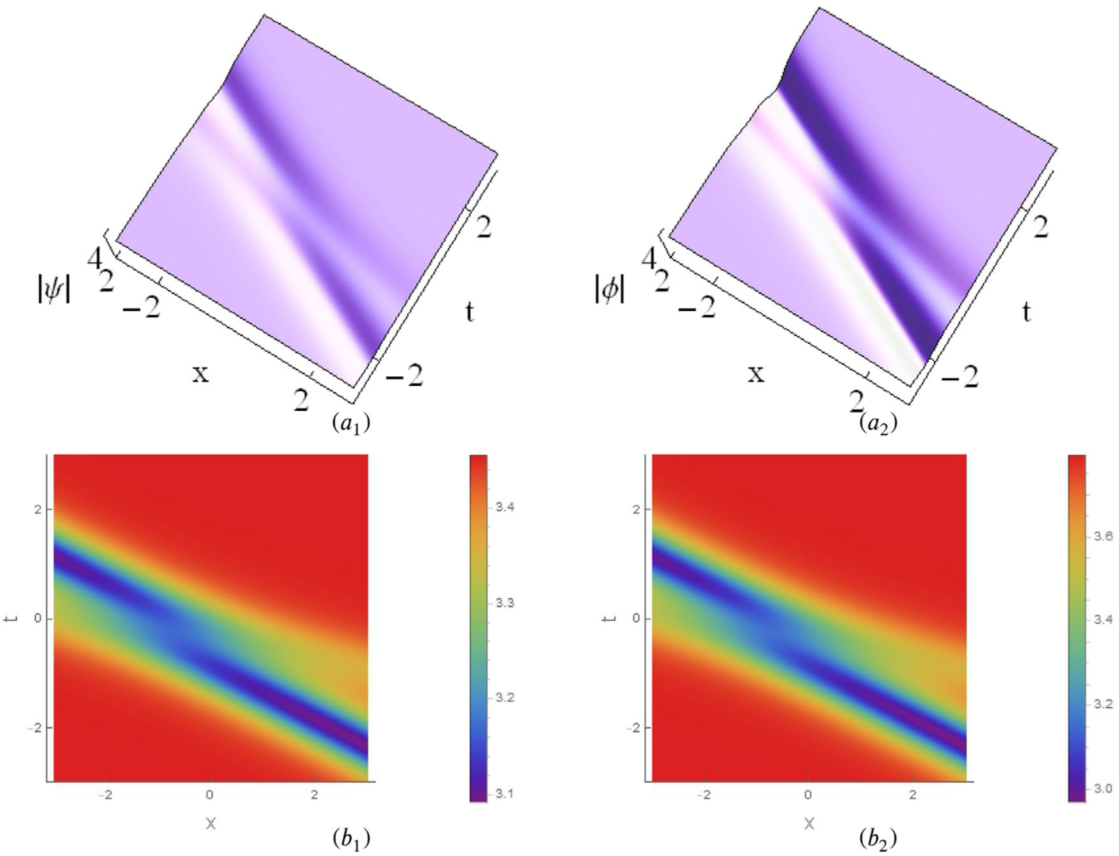

FIGURE 9 Interaction between the dark-dark two solitons via Solutions (10) at $y = 0$ with $\mu = 2\sqrt{\frac{170}{57}}$, $\nu = 2\sqrt{\frac{205}{57}}$, $p_1 = 2 + \frac{1}{2}i$, $p_2 = 1 + i$, $\alpha_1 = 1$, $\alpha_2 = 2\sqrt{3}$, $\beta_1 = 1$, $\beta_2 = \sqrt{3}$, $k = -0.5$, $l = -\frac{\sqrt{3}}{2}$ and $\xi_{10} = 0$

4 | BRIGHT-BRIGHT SOLITON SOLUTIONS AND SOLITON INTERACTION FOR SYSTEM (2)

4.1 | Bright-bright soliton solutions for System (2)

Under the variable transformations [49]

$$\psi = \frac{g}{f}, \quad \phi = \frac{h}{f},$$

with $\sigma = 1$, System (2) can be transformed into

$$(iD_t + D_x^2 + D_y^2)g \cdot f = 0, \tag{12a}$$

$$(iD_t + D_x^2 + D_y^2)h \cdot f = 0, \tag{12b}$$

$$(D_x^2 + D_y^2)f \cdot f = |g|^2 + |h|^2. \tag{12c}$$

N-bright-bright soliton solutions in terms of the Gramian for System (2) are

$$\psi = \frac{g}{f}, \quad \phi = \frac{h}{f}, \tag{13}$$

where

$$f = \begin{vmatrix} \mathbf{A} & \mathbf{I} \\ -\mathbf{I} & \tilde{\mathbf{B}} \end{vmatrix}, \quad g = \begin{vmatrix} \mathbf{A} & \mathbf{I} & \mathbf{\Phi}^T \\ -\mathbf{I} & \tilde{\mathbf{B}} & \mathbf{0}^T \\ \mathbf{0} & \mathbf{\Psi}^{(1)} & 0 \end{vmatrix}, \quad h = \begin{vmatrix} \mathbf{A} & \mathbf{I} & \mathbf{\Phi}^T \\ -\mathbf{I} & \tilde{\mathbf{B}} & \mathbf{0}^T \\ \mathbf{0} & \mathbf{\Psi}^{(2)} & 0 \end{vmatrix},$$

$\tilde{\mathbf{B}}$ is the $N \times N$ matrice whose elements are $\tilde{b}_{mn}$'s, $\mathbf{\Phi}$, $\mathbf{\Psi}^{(1)}$ and $\mathbf{\Psi}^{(2)}$ are the $1 \times N$ matrices, with

$$\begin{aligned} a_{mn} &= \frac{1}{p_m + p_n^*} e^{\xi_m + \xi_n^*}, \quad \tilde{b}_{mn} = \frac{\alpha_m^{(1)*}\alpha_n^{(1)} + \alpha_m^{(2)*}\alpha_n^{(2)}}{2(p_m^* + p_n)}, \\ \mathbf{\Psi}^{(1)} &= -(\alpha_1^{(1)}, \alpha_2^{(1)}, \dots, \alpha_N^{(1)}), \quad \mathbf{\Psi}^{(2)} = -(\alpha_1^{(2)}, \alpha_2^{(2)}, \dots, \alpha_N^{(2)}), \\ \mathbf{\Phi} &= (e^{\xi_1}, e^{\xi_2}, \dots, e^{\xi_N}), \quad \xi_n = p_n(kx + ly) + ip_n^2 t + \xi_{n0}, \end{aligned}$$

which satisfies $k^2 + l^2 = 1$, and $\alpha_n^{(1)}$'s, $\alpha_n^{(2)}$'s are the complex constants.

Setting $N = 2$ in Solutions (13), we derive the bright-bright two-soliton solutions for System (2),

$$\psi = \frac{g}{f}, \quad \phi = \frac{h}{f}, \tag{14}$$

where

$$\begin{aligned} f &= 1 + e^{\xi_1 + \xi_1^* + \tilde{\omega}_{11}} + e^{\xi_1 + \xi_2^* + \tilde{\omega}_0} + e^{\xi_2 + \xi_1^* + \tilde{\omega}_0^*} + e^{\xi_2 + \xi_2^* + \tilde{\omega}_{22}} + e^{\xi_1 + \xi_1^* + \xi_2 + \xi_2^* + \tilde{\omega}_{33}}, \\ g &= \alpha_1^{(1)} e^{\xi_1} + \alpha_2^{(1)} e^{\xi_2} + e^{\xi_1 + \xi_2 + \xi_1^* + \tilde{\omega}_{12}} + e^{\xi_1 + \xi_2 + \xi_2^* + \tilde{\omega}_{21}}, \\ h &= \alpha_1^{(2)} e^{\xi_1} + \alpha_2^{(2)} e^{\xi_2} + e^{\xi_1 + \xi_2 + \xi_1^* + \tilde{\tilde{\omega}}_{12}} + e^{\xi_1 + \xi_2 + \xi_2^* + \tilde{\tilde{\omega}}_{21}}, \end{aligned}$$

with

$$\begin{aligned} e^{\tilde{\omega}_{11}} &= \frac{b_{11}}{p_1 + p_1^*}, \quad e^{\tilde{\omega}_0} = \frac{b_{21}}{p_1 + p_2^*}, \quad e^{\tilde{\omega}_{22}} = \frac{b_{22}}{p_2 + p_2^*}, \\ e^{\tilde{\omega}_{33}} &= \frac{|p_1 - p_2|^2}{(p_1 + p_1^*)(p_2 + p_2^*)|p_1 + p_2^*|^2}(b_{11}b_{22} - b_{12}b_{21}), \\ e^{\tilde{\omega}_{12}} &= \frac{p_1 - p_2}{(p_1 + p_1^*)(p_2 + p_1^*)}\left(\alpha_1^{(1)} b_{12} - \alpha_2^{(1)} b_{11}\right), \\ e^{\tilde{\omega}_{21}} &= \frac{p_2 - p_1}{(p_1 + p_2^*)(p_2 + p_2^*)}\left(\alpha_2^{(1)} b_{21} - \alpha_1^{(1)} b_{22}\right), \end{aligned}$$

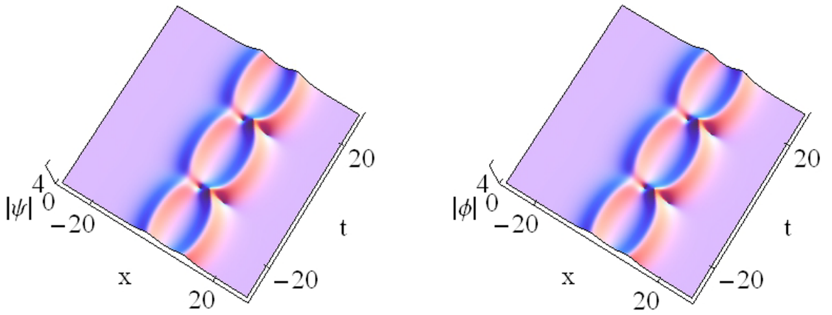

FIGURE 10 Bound-state bright-bright solitons via Solutions (14) at $y = 0$ with $p_1 = 0.85$, $p_2 = 1$, $k = 0.5$, $l = \frac{\sqrt{3}}{2}$, $\alpha_1^{(1)}=\alpha_1^{(2)}=\alpha_2^{(1)}=\alpha_2^{(2)}=1$, $\xi_{10} = 1.5$ and $\xi_{20} = 1$

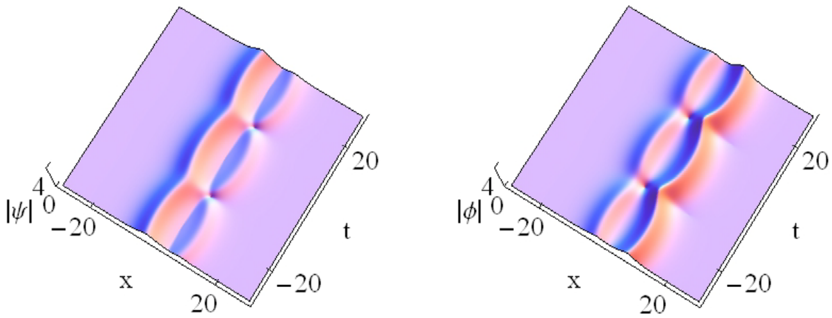

FIGURE 11 The same as Figure 10 except that $\alpha_1^{(1)} = 1.5$

$$e^{\tilde{\omega}_{12}} = \frac{p_1 - p_2}{(p_1 + p_1^*)(p_2 + p_1^*)}\left(\alpha_1^{(2)} b_{12} - \alpha_2^{(2)} b_{11}\right),$$
$$e^{\tilde{\omega}_{21}} = \frac{p_2 - p_1}{(p_1 + p_2^*)(p_2 + p_2^*)}\left(\alpha_2^{(2)} b_{21} - \alpha_1^{(2)} b_{22}\right).$$

Setting $N = 3$ in Solutions (13), we derive the bright-bright three-soliton solutions for System (2) with

$$f = \begin{vmatrix} a_{11} & a_{12} & a_{13} & 1 & 0 & 0 \\ a_{21} & a_{22} & a_{23} & 0 & 1 & 0 \\ a_{31} & a_{32} & a_{33} & 0 & 0 & 1 \\ -1 & 0 & 0 & \tilde{b}_{11} & \tilde{b}_{12} & \tilde{b}_{13} \\ 0 & -1 & 0 & \tilde{b}_{21} & \tilde{b}_{22} & \tilde{b}_{23} \\ 0 & 0 & -1 & \tilde{b}_{31} & \tilde{b}_{32} & \tilde{b}_{33} \end{vmatrix}, \quad g = \begin{vmatrix} a_{11} & a_{12} & a_{13} & 1 & 0 & 0 & e^{\xi_1} \\ a_{21} & a_{22} & a_{23} & 0 & 1 & 0 & e^{\xi_2} \\ a_{31} & a_{32} & a_{33} & 0 & 0 & 1 & e^{\xi_3} \\ -1 & 0 & 0 & \tilde{b}_{11} & \tilde{b}_{12} & \tilde{b}_{13} & 0 \\ 0 & -1 & 0 & \tilde{b}_{21} & \tilde{b}_{22} & \tilde{b}_{23} & 0 \\ 0 & 0 & -1 & \tilde{b}_{31} & \tilde{b}_{32} & \tilde{b}_{33} & 0 \\ 0 & 0 & 0 & -\alpha_1^{(1)} & -\alpha_2^{(1)} & -\alpha_3^{(1)} & 0 \end{vmatrix},$$

$$h = \begin{vmatrix} a_{11} & a_{12} & a_{13} & 1 & 0 & 0 & e^{\xi_1} \\ a_{21} & a_{22} & a_{23} & 0 & 1 & 0 & e^{\xi_2} \\ a_{31} & a_{32} & a_{33} & 0 & 0 & 1 & e^{\xi_3} \\ -1 & 0 & 0 & \tilde{b}_{11} & \tilde{b}_{12} & \tilde{b}_{13} & 0 \\ 0 & -1 & 0 & \tilde{b}_{21} & \tilde{b}_{22} & \tilde{b}_{23} & 0 \\ 0 & 0 & -1 & \tilde{b}_{31} & \tilde{b}_{32} & \tilde{b}_{33} & 0 \\ 0 & 0 & 0 & -\alpha_1^{(2)} & -\alpha_2^{(2)} & -\alpha_3^{(2)} & 0 \end{vmatrix}.$$

4.2 | Discussion on the bright-bright solitons for System (2)

Figures 10 and 11 depict the bound-state bright-bright solitons via Solutions (14). Bound-state solitons in Figure 10 evolves with the periodic attraction and repulsion, and we can observe that the profiles of the ψ and ϕ components have the same form. Figure 11 depicts the asymmetric bound-state bright-bright solitons with $\alpha_1^{(1)} = 1.5$.

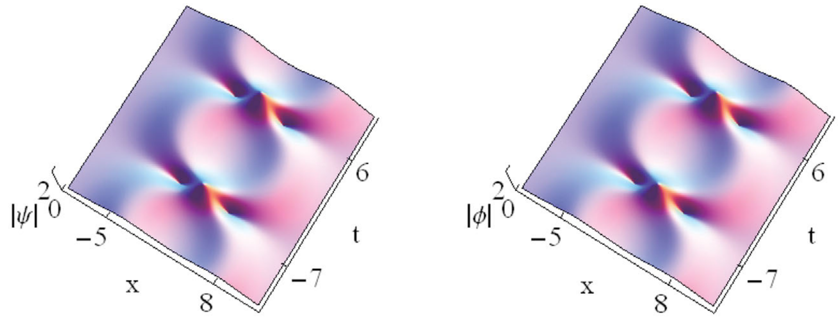

FIGURE 12 The same as Figure 10 except that $p_1 = 0.65$, $\xi_{10} = 1$

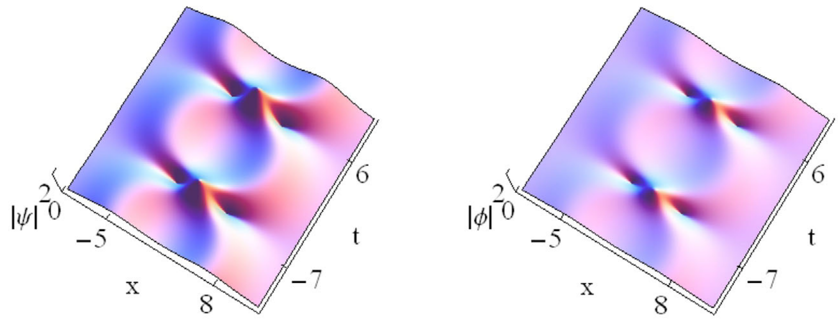

FIGURE 13 The same as Figure 11 except that $\alpha_1^{(1)} = \alpha_1^{(2)} = 2$

Figures 12 and 13 depict the bound-state bright-bright solitons via Solutions (14), indicating that a bound-state soliton undergoes an enhancement between each two cycles and evolves periodically.

Figure 14 depicts a soliton complex with the periodic oscillation. Unlike the bound-state solitons in Figures 10-13, the soliton complex in Figure 14 does not form the cycles. Figure 15 presents the soliton complex with the energy switching properties, and such nonlinear switching behavior is related to applied in the ultra-fast logic gates using asymmetric fiber couplers [56].

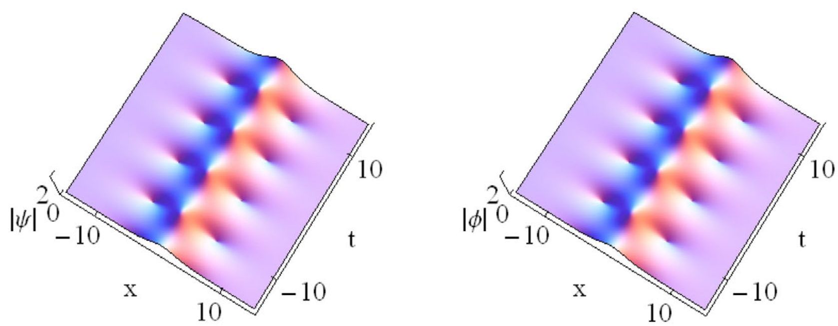

FIGURE 14 Soliton complex via Solutions (14) at $y = 0$ with the same values of parameters as Figure 10 except that $p_1 = 0.2$, $\xi_{10} = 0$

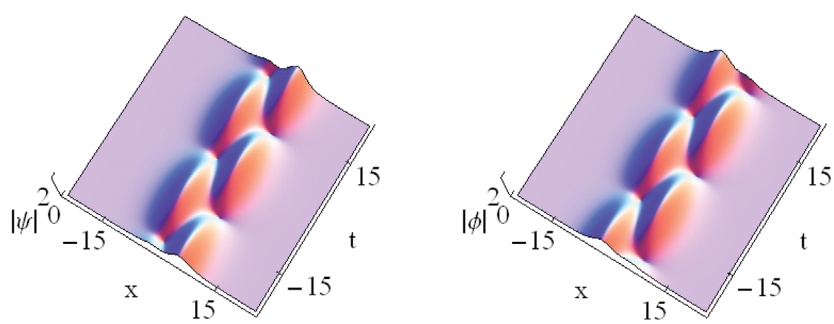

FIGURE 15 Soliton complex via Solutions (14) at $y = 0$ with the same values of parameters as Figure 10 except that $\alpha_1^{(1)} = -1$, $\xi_{10} = 1.2$

5 CONCLUSIONS

In this paper, we have investigated the (2 + 1)-dimensional coupled nonlinear Schrödinger system, that is, System (2), which describes the propagation of the optical soliton through the Kerr nonlinear fiber in which each component diffracts in two transverse dimensions. Based on the KP hierarchy reduction, bright, dark and mixed vector soliton solutions in terms of the Gramian for System (2) have been derived, that is, Solutions (4), (8) and (13). According to such solutions, investigations on the vector solitons have been performed, as follows:

(1) For the bright-dark solitons: Figures 1 and 2 have depicted the one solitons whose ϕ component is gray or black. Figure 3 have depicted the interactions between the two solitons, with the bouncing effect emerged when $p_{1R}=p_{2R}$, as seen in Figure 3b. Beating effect has appeared during the interaction where the two solitons form a bound mode when $t \to 0$, as seen in Figure 4. In Figure 5, oscillating effect has enhanced around the interaction area. Figure 6 has depicted the breathing effect during the interaction, with the moving and stationary bound-state two solitons presented. We have concluded that the interaction between the bright-dark solitons is elastic.
(2) For the dark-dark solitons: When $k\alpha_1 + l\alpha_2 = k\beta_1 + l\beta_2$, degenerate dark-dark one solitons have been derived in Figure 7, whereas non-degenerate dark-dark solitons have been derived with $k\alpha_1 + l\alpha_2 \neq k\beta_1 + l\beta_2$ in Figure 8. Figure 9 has depicted the interaction between two solitons. During the interaction, the two solitons have been seen to keep their amplitudes and velocities invariant except for some phase shifts.
(3) For the bright-bright solitons: Figures 10 and 11 have depicted the bound-state solitons which evolve with the periodic attraction and repulsion. Profiles of the ψ and ϕ components have been the same, while asymmetric bound-state bright-bright solitons have been depicted in Figure 11. Bound-state solitons in Figures 12 and 13 have undergone the enhancement between each two cycles and evolved periodically. Figure 14 has depicted a soliton complex with the periodic oscillating and Figure 15 has presented the soliton complex with the energy switching properties.

ACKNOWLEDGEMENTS

We express our sincere thanks to the Editors and Reviewers for their valuable comments. This work has been supported by the National Natural Science Foundation of China under Grant Nos. 11772017, 11805020, 11272023 and 11471050, by the Fund of State Key Laboratory of Information Photonics and Optical Communications (Beijing University of Posts and Telecommunications), China (IPOC: 2017ZZ05), by the Fundamental Research Funds for the Central Universities of China under Grant No. 2011BUPTYB02, and by the Fundamental Research Funds for the Central Universities in UIBE (CXTD12-04).

CONFLICT OF INTEREST

The authors declare no potential conflict of interests.

ORCID

Yu-Qiang Yuan https://orcid.org/0000-0002-9836-4966

REFERENCES

[1] Agrawal, G.P.: Nonlinear Fiber Optics, Academic, New York (1995)
[2] Ding, C.C., Gao, Y.T., Deng, G.F., Wang, D.: Lax pair, conservation laws, Darboux transformation, breathers and rogue waves for the coupled nonautonomous nonlinear Schrödinger system in an inhomogeneous plasma. Chaos Solitons Fract. 133, 109580 (2020)
[3] Liu, D.Y., Sun, W.R.: Rational solutions for the nonlocal sixth-order nonlinear Schrödinger equation. Appl. Math. Lett. 84, 63 (2018)
[4] Liu, D.Y., Yu, H.M.: Mixed localized wave solutions of the Hirota equation. Appl. Math. Lett. 118, 107154 (2021)
[5] Liu, W.J., Pang, L.H., Yan, H., Ma, G.L., Lei, M., Wei, Z.Y.: Bidirectional all-optical switches based on highly nonlinear optical fibers. Epl 116, 64002 (2016)
[6] Jia, T.T., Gao, Y.T., Deng, G.F., Hu, L.: Quintic time-dependent-coefficient derivative nonlinear Schrödinger equation in hydrodynamics or fiber optics: bilinear forms and dark/anti-dark/gray solitons. Nonlinear Dyn. 98, 269 (2019)
[7] Yan, Y.Y., Liu, W.J., Zhou, Q., Biswas, A.: Dromion-like structures and periodic wave solutions for variable-coefficients complex cubic-quintic Ginzburg-Landau equation influenced by higher-order effects and nonlinear gain. Nonlinear Dyn. 99, 1313 (2020)
[8] Fan, X.Y., Qu, T.Q., Huang, S.C. et al.: Analytic study on the influences of higher-order effects on optical solitons in fiber laser. Optik 186, 326 (2019)
[9] Liu, W.J., Pang, L.H., Han, H.N. et al.: Dark solitons in WS_2 erbium-doped fiber lasers. Photon. Res. 4(3), 111 (2016)

[10] Liu, W.J., Yu, W.T., Yang, C.Y. et al.: Analytic solutions for the generalized complex Ginzburg-Landau equation in fiber lasers. Nonlinear Dyn. 89, 2933 (2017)
[11] Wang, C.J., Nie, Z.Z., Xie, W.J. et al.: Dark soliton control based on dispersion and nonlinearity for third-order nonlinear Schrödinger equation. Optik 184, 370 (2019)
[12] Liu, W.J., Pang, L.H., Han, H.N. et al.: Tungsten disulphide for ultrashort pulse generation in all-fiber lasers. Nanoscale 9, 5806 (2017)
[13] Liu, W.J., Pang, L.H., Han, H.N. et al.: Tungsten disulfide saturable absorbers for 67 fs mode-locked erbium-doped fiber lasers. Opt. Express 25, 2590 (2017)
[14] Liu, W.J., Zhu, Y.N., Liu, M.L. et al.: Optical properties and applications for MoS_2-Sb_2Te_3-MoS_2 heterostructure materials. Photon. Res. 6(3), 220 (2018)
[15] Gao, X.Y., Guo, Y.J., Shan, W.R.: Water-wave symbolic computation for the Earth, Enceladus and Titan: The higher-order Boussinesq-Burgers system, auto- and non-auto-Bäcklund transformations. Appl. Math. Lett. 104, 106170 (2020)
[16] Gao, X.Y., Guo, Y.J., Shan, W.R.: Shallow water in an open sea or a wide channel: Auto- and non-auto-Bäcklund transformations with solitons for a generalized (2+1)-dimensional dispersive long-wave system. Chaos Solitons Fract. 138, 109950 (2020)
[17] Feng, Y.J., Gao, Y.T., Li, L.Q., Jia, T.T.: Bilinear form, solitons, breathers and lumps of a (3+1)-dimensional generalized Konopelchenko-Dubrovsky-Kaup-Kupershmidt equation in ocean dynamics, fluid mechanics and plasma physics. Eur. Phys. J. Plus 135, 272 (2020)
[18] Feng, Y.J., Gao, Y.T., Jia, T.T., Li, L.Q.: Soliton interactions of a variable-coefficient three-component AB system for the geophysical flows. Mod. Phys. Lett. B 33, 1950354 (2019)
[19] Su, J.J., Gao, Y.T., Deng, G.F., Jia, T.T.: Solitary waves, breathers, and rogue waves modulated by long waves for a model of a baroclinic shear flow. Phys. Rev. E 100, 042210 (2019)
[20] Su, J.J., Gao, Y.T., Ding, C.C.: Darboux transformations and rogue wave solutions of a generalized AB system for the geophysical flows. Appl. Math. Lett. 88, 201 (2019)
[21] Hu, L., Gao, Y.T., Jia, S.L., Su, J.J., Deng, G.F.: Solitons for the (2+1)-dimensional Boiti-Leon-Manna-Pempinelli equation for an irrotational incompressible fluid via the Pfaffian technique. Mod. Phys. Lett. B 33, 1950376 (2019)
[22] Hu, L., Gao, Y.T., Jia, T.T., Deng, G.F., Li, L.Q.: Higher-order hybrid waves for the (2+1)-dimensional Boiti-Leon-Manna-Pempinelli equation for an irrotational incompressible fluid via the modified Pfaffian technique. Z. Angew. Math. Phys. 72, 75 (2021)
[23] Jia, T.T., Gao, Y.T., Yu, X., Li, L.Q.: Darboux transformation, bilinear forms and solitonic interactions for a combined Calogero-Bogoyavlenskii-Schiff-type equation. Appl. Math. Lett. 114, 106702 (2021)
[24] Deng, G.F., Gao, Y.T., Ding, C.C., Su, J.J.: Solitons and breather waves for the generalized Konopelchenko-Dubrovsky-Kaup-Kupershmidt system in fluid mechanics, ocean dynamics and plasma physics. Chaos Solitons Fract. 140, 110085 (2020)
[25] Deng, G.F., Gao, Y.T., Su, J.J., Ding, C.C., Jia, T.T.: Solitons and periodic waves for the (2+1)-dimensional generalized Caudrey-Dodd-Gibbon-Kotera-Sawada equation in fluid mechanics. Nonlinear Dyn. 99, 1039 (2020)
[26] Li, L.Q., Gao, Y.T., Hu, L., Jia, T.T., Ding, C.C., Feng, Y.J.: Bilinear form, soliton, breather, lump and hybrid solutions for a (2+1)-dimensional Sawada-Kotera equation. Nonlinear Dyn. 100, 2729 (2020)
[27] Ding, C.C., Gao, Y.T., Deng, G.F.: Breather and hybrid solutions for a generalized (3+1)-dimensional B-type Kadomtsev-Petviashvili equation for the water waves. Nonlinear Dyn. 97, 2723 (2019)
[28] Liu, F.Y., Gao, Y.T., Yu, X., Ding, C.C., Deng, G.F., Jia, T.T.: Painlevé analysis, Lie group analysis and soliton-cnoidal, resonant, hyperbolic function and rational solutions for the modified Korteweg-de Vries-Calogero-Bogoyavlenskii-Schiff equation in fluid mechanics. Chaos Solitons Fract. 144, 110559 (2021); Liu, F.Y., Gao, Y.T., Yu, X., Li, L.Q., Ding, C.C., Wang, D.: Lie group analysis and analytic solutions for a (2+1)-dimensional generalized Bogoyavlensky-Konopelchenko equation in fluid mechanics and plasma physics. Eur. Phys. J. Plus (2021) in press, Ms. No. EPJP-D-20-03633R2; Du, Z., Ma, Y.P., Beak-shaped rogue waves for a higher-order coupled nonlinear Schrödinger system with 4×4 Lax pair, Appl. Math. Lett. 116, 106999 (2021)
[29] Chen, Z.G., Segev, M., Coskun, T.H., Christodoulides, D.N., Afanasjev, V.V.: Incoherently Coupled Photorefractive Spatial Soliton Pairs. J. Opt. Soc. Am. B 14, 3066 (1997)
[30] Afanasjev, V.V., Kivshar, Y.S., Konotop, V.V., Serkin, V.N.: Dynamics of coupled dark and bright optical solitons. Opt. Lett. 14, 805 (1989)
[31] Seve, E., Millot, G., Wabnitz, S.: Buildup of terahertz vector dark-soliton trains from induced modulation instability in highly birefringent optical fiber. Opt. Lett. 23, 1829 (1998)
[32] Gupta, R.K., Kumar, V., Jiwari, R.: Exact and numerical solutions of coupled short pulse equation with time-dependent coefficients. Nonlinear Dyn. 79, 455 (2015)
[33] Lü, X., Ling, L.M.: Vector bright solitons associated with positive coherent coupling via Darboux transformation. Chaos 25, 123103 (2015)
[34] Ohta, Y., Wang, D.S., Yang, J.: General N-Dark-Dark Solitons in the Coupled Nonlinear Schrödinger Equations. Stud. Appl. Math. 127, 345 (2011)
[35] Zhang, H.Q.: Energy-exchange collisions of vector solitons in the N-coupled mixed derivative nonlinear Schrödinger equations from the birefringent optical fibers. Opt. Commun. 290, 141 (2013)
[36] Feng, B.F.: General N-soliton solution to a vector nonlinear Schrödinger equation. J. Phys. A 47, 355203 (2014)
[37] Manikandan, N., Radhakrishnan, R., Aravinthan, K.: Generalized dark-bright vector soliton solution to the mixed coupled nonlinear Schrödinger equations. Phys. Rev. E 90, 022902 (2014)
[38] Rand, D., Glesk, I., Brès, C.S.: et al, Observation of temporal vector soliton propagation and collision in birefringent fiber. Phys. Rev. Lett. 98, 053902 (2007)
[39] Kivshar, Y.S., Agrawal, G.P.: Optical Solitons, Academic, San Diego (2003)

[40] Trillo, S., Toruellas, W.: Spatial Solitons, Springer, Berlin (2001)
[41] Manakov, S.V.: On the theory of two-dimensional stationary self-focusing electromagnetic waves. Zh. Eksp. Teor. Fiz. 65, 505 (1973)
[42] Manakov, S.V.: On the theory of two-dimensional stationary self-focusing of electromagnetic waves. Sov. Phys. JETP 38, 248 (1974)
[43] Chen, S.H., Mihalache, D.: Vector rogue waves in the Manakov system: diversity and compossibility. J. Phys. A 48, 215202 (2015)
[44] Zhai, B.G., Zhang, W.G., Wang, X.L., Zhang, H.Q.: Multi-rogue waves and rational solutions of the coupled nonlinear Schrödinger equations. Nonlinear Anal. 14, 14 (2013)
[45] Menyuk, C.R.: Nonlinear pulse propagation in birefringent optical fibers. IEEE J. Quantum Elect. 23, 174 (1987)
[46] Kang, J.U., Stegeman, G.I., Aitchison, J.S., Akhmediev, N.: Observation of Manakov spatial solitons in AlGaAs planar waveguides. Phys. Rev. Lett. 76, 3699 (1996)
[47] Bélanger, P.A., Paré, C.: Soliton switching and energy coupling in two-mode fibers: analytical results. Phys. Rev. A 41, 5254 (1990)
[48] Radhakrishnan, R., Aravinthan, K.: A dark-bright optical soliton solution to the coupled nonlinear Schrödinger equation. J. Phys. A 40, 13023 (2007)
[49] Zhang, H.Q., Meng, X.H., Xu, T., Li, L.L., Tian, B.: Interactions of bright solitons for the (2+ 1)-dimensional coupled nonlinear Schrödinger equations from optical fibres with symbolic computation. Phys. Scr. 75, 537 (2007)
[50] Malmberg, J.N., Carlsson, A.H., Anderson, D., Lisak, M.: Vector solitons in (2+1) dimensions. Opt. Lett. 25, 643 (2000)
[51] Kivshar, Y.S., Agrawal, G.P.: Optical Solitons from Fibers to Photonic Crystals, Academic, San Diego (2003)
[52] Jimbo, M., Miwa, T.: Solitons and infinite dimensional Lie algebras. Publ RIMS, Kyoto Univ. 19, 943 (1983)
[53] Chen, J.C., Chen, Y., Feng, B.F., Maruno, K.: General mixed multi-soliton solutions to one-dimensional multicomponent Yajima-Oikawa system. J. Phys. Soc. Jpn. 84, 074001 (2015)
[54] Yu, G.F., Xu, Z.W., Hu, J., Zhao, H.Q.: Bright and dark soliton solutions to the AB system and its multi-component generalization. Commun. Nonlinear Sci. Numer. Simulat. 47, 178 (2017)
[55] Hirota, R.: The Direct Method in Soliton Theory, Cambridge Univ. Press, Cambridge (2004)
[56] Agrawal, G.P.: Applications of Nonlinear Fiber Optics, Academic, San Diego (2001)

How to cite this article: Sun, Y., Tian, B., Qu, Q.-X., Chai, H.-P., Yuan, Y.-Q., Shan, W.-R., Jiang, Y. Vector solitons for the (2+1)-dimensional coupled nonlinear Schrödinger equations in the Kerr nonlinear optical fiber. *Z Angew Math Mech*. 2021;e202000232. https://doi.org/10.1002/zamm.202000232